Mapping the self-association domains of ataxin-1:

Identification of novel non overlapping motifs

Rajesh P Menon*[1], Daniel Soong[2,3,4], Cesira de Chiara[1], Mark Holt[2], John E McCormick[1], N Anilkumar[3] and Annalisa Pastore*[5]

[1] MRC National Institute for Medical Research, The Ridgeway, London NW7 1AA UK

[2] Randall Division for Cell and Molecular Biophysics, New Hunt's House, King's College London, Guy's Campus, London, SE1 1UL

[3] British Heart Foundation Centre of Research Excellence, King's College London, Denmark Hill Campus, London, SE5 9NU

[4] Present address: MRC Centre for Reproductive Health, Queen's Medical Research Institute, University of Edinburgh, 47 Little France Crescent, Edinburgh EH16 4TJ

[5] Department of Molecular Neuroscience, Institute of Psychiatry, King's College London, Denmark Hill Campus, London, SE5 9NU

*To whom correspondence should be sent

Running title: Mapping the self-association domains of ataxin-1

Keywords: confocal microscopy, foci, FRET, misfolding diseases, spinocerebellar ataxia type 1

Abstract

The neurodegenerative spinocerebellar ataxia type 1 (SCA1) is caused by aggregation and misfolding of the ataxin-1 protein. While the pathology correlates with mutations that lead to expansion of a polyglutamine tract in the protein, other regions contribute to the aggregation process as also non-expanded ataxin-1 is intrinsically aggregation-prone and forms nuclear foci in cell. Here, we have used a combined approach based on FRET analysis, confocal microscopy and *in vitro* techniques to map aggregation-prone regions other than polyglutamine and to establish the importance of dimerization in self-association/foci formation. Identification of aggregation-prone regions other than polyglutamine could greatly help the development of SCA1 treatment more specific than that based on targeting the low complexity polyglutamine region.

Introduction

The inherited disease spinocerebellar ataxia type 1 (SCA1) is an autosomal dominant neurodegenerative pathology characterized by progressive loss of Purkinje cells in the cerebellar cortex and of neurons in the spinocerebellum (Zoghbi & Orr, 1995; Cummings, Orr & Zoghbi, 1999; Matilla-Dueñas, Goold & Giunti 2008). The pathogenic mechanism of SCA1, presently incurable, seems to be complex (de Chiara & Pastore, 2014). It is thought to be caused by aggregation and misfolding of ataxin-1 that is associated to expansion of a polymorphic polyglutamine (polyQ) tract in the N-terminus of the protein (Orr, et al., 1993; Cummings et al., 1998; Klement et al., 1998; de Chiara et al., 2005, Mizutani, et al., 2005; Tsuda et al., 2005; Lam, et al., 2006). A similar mechanism triggers the aggregation of a larger family of polyQ containing proteins such as the better known Huntington's chorea (Arrasate & Finkbeiner, 2012). For all members of this disease family, polyQ expansion seems to be the necessary event for disease development (Verbeek & Warrenburg, 2011; Robertson & Bottomley, 2012; Blum, Schwendeman & Shaham, 2013; Menon et al., 2013). It is however an accepted concept that regions outside the polyQ tracts significantly contribute to the aggregation process urging the importance of studying protein context and analysing the behaviour of regions of these proteins also sequence-wise distant from the polyQ tract (Masino et al., 2004; de Chiara et al., 2005; Ellisdon et al., 2006; Gales et al., 2005).

In agreement with this view, ataxin-1 is an intrinsically aggregation-prone protein known to form, also in its non-expanded form, diffuse cellular aggregates some time named foci (Matilla et al., 1997; Tsai et al 2004; Menon et al., 2005; de Chiara et al., 2005; Osmand et al., 2006; Menon et al., 2012). The number and size of foci increases in the presence of polyQ expansion. A self-association region of the non-expanded protein was mapped in the centre of the protein and identified to overlap the only certified globular domain of the otherwise

mostly unstructured protein, the AXH domain that spans residues 562-689 (SMART SM00536) (Burright et al., 1997; de Chiara et al., 2003). This motif is functionally very important as it is involved in transcriptional regulation as well as in the RNA-binding activity of ataxin-1 (Matilla et al., 1997; Okazawa et al 2002; Tsai et al., 2004; de Chiara et al., 2003; de Chiara et al., 2005; Mizutani et al., 2005; Tsuda et al 2005; Lam et al., 2006; Serra et al., 2006; Goold et al., 2007; Lee et al 2011). AXH is also necessary and sufficient for the majority of the known interactions of ataxin-1 with other proteins, most of which are transcriptional regulators (Tsai et al., 2004; Tsuda et al 2005; Lam et al., 2006; Goold et al., 2007; Serra et al., 2006). Although AXH does not contain a polyQ tract and is sequence-wise distant from it, it seems to play an important role in ataxin-1 aggregation. In solution, the isolated AXH forms a complex equilibrium between monomer, dimer, tetramer and higher molecular weight species (de Chiara et al., 2013a). This process was suggested to be on-pathway to protein aggregation and fibre formation. Deletion of the AXH domain leads to reduction of intra-nuclear foci formation by expanded ataxin-1 in eukaryotic cells (de Chiara et al., 2005).

Realization that ataxin-1 aggregation may be triggered by more than one region has suggested that this behaviour could inspire the development of new drugs that could target regions other than or in addition to the polyQ tract. Such drugs would be potentially more specific than compounds preventing the aggregation of the low complexity polyQ. A recent report has for instance shown that blockage of the AXH domain into a monomeric species by binding it to a peptide from the natural partner protein Capicua (CIC) prevents the aggregation and misfolding of the isolated domain (de Chiara et al., 2013a; de Chiara et al., 2013b). If the same held true also for the full-length protein, this strategy would have terrific consequences for the design of novel therapeutic lead compounds. To follow up this strategy, however, more information about the regions responsible for self-association is needed.

Here, we have combined studies in cell using confocal microscopy as well as FRET (Förster Resonance Energy Transfer) analysis and *in vitro* investigations of isolated regions of ataxin-1 to map the regions necessary/sufficient for foci formation and explore the relationship between dimerization and self-association of non-expanded ataxin-1. FRET based approaches have proven to be a powerful tool for the analysis of protein homo-dimerization in cells (Itoh et al., 2011; Placone & Hristova, 2012; Hlavackova et al., 2012). Our results establish the existence of dual non-overlapping self-association motifs within ataxin-1 reinforcing the importance of the AXH domain in dimerization/aggregation. We also demonstrate that destabilization of AXH dimerization appreciably reduces protein self-association. This evidence may pave the way to new directions towards the development of anti-SCA1 drug design.

Materials and Methods

Plasmids, cell culture, transfections and Imaging

Non-expanded (Q30) ataxin-1 and truncated ataxin-1 fusion proteins were constructed in pEYFP or pECFP vectors using the standard PCR and mutagenesis methods previously established in our laboratory (Menon et al., 2012). COS cells were grown in chamber slides in Dulbecco's modified Eagle medium supplemented with 10% fetal bovine serum and 100 U/mL penicillin-streptomycin (Invitrogen Life Technologies). Cells were transfected with appropriate plasmid DNA using GeneCellin tranfection reagent (BioCellChallenge). Cells were fixed using 4% paraformaldehyde 54 h post-transfection and slides were mounted using CitiFluor (Agar Scientific). Cells were observed and recorded using a laser scanning confocal microscope (de Chiara et al., 2009).

Analytical Size Exclusion Chromatography

Size exclusion chromatography was performed using a prepacked Superdex-75™ 10/300 GL column (Pharmacia) equilibrated with a 20 mM Tris-HCl pH 7, 150 mMNaCl, 1 mM TCEP buffer solution. Aliquotes of 200 µl of 150 µM AXH and TLND2AXHincubated for 24h at 37°Cin 20 mMpH 7, 150 mMNaCl, 1 mM TCEP wereinjected separately and eluted using a 0.8 ml/min flow rate. Albumin (67 kDa), Ovalbumin (43 kDa), Carbonic anhydrase (29 kDa), and Ribonuclease A (13.7 kDa) were used as standards for the molecular mass, whereas the Blue Dextran 2000 was used for the determination of the void volume of the column.

FRET Microscopy

Samples for FRET were imaged on a Zeiss LSM 510 confocal microscope using a 63x 1.4NA Plan NeoFluar oil immersion objective and FRET analysis was carried out as previously described in detail (Menon et al., 2012). Pre- and post-bleach CFP and YFP images were imported into Mathematica 7.0 for processing as described (Matthews et al., 2008). Briefly, images were smoothed using a 3x3 box mean filter, background subtracted, and post-bleach images fade compensated.

$$E = \frac{CFPpostbleach - CFPprebleach}{CFPpostbleach}$$

FRET efficiencies were then extracted from pixels falling inside the bleach region and plotted against the bleach efficiency on a pixel-by-pixel basis. FRET efficiency showed a linear correlation with bleach efficiency enabling determination of FRET efficiency at 100 % bleach efficiency by extrapolation. Data from images were used only if YFP bleaching efficiency was greater than 50%. Finally, the FRET efficiency was converted in to the inter-fluorophore radius using:

$$r = Ro \sqrt[6]{\frac{1}{E} - 1}$$

where Ro is the Foerster radius for CFP and YFP, which is 4.95 nm.

Results

Ataxin-1 foci formation is independent of polyQ and mediated by the C-terminus

We first explored the relationship between foci formation and polyQ in non-expanded ataxin-1. We used non-expanded ataxin-1 to be able to detect the intrinsic properties of the functional protein that could then be transferred to the expanded form. We created several deletion constructs for expression analysis in mammalian cells in which the protein was N-terminally attached to the yellow fluorescent protein (YFP) (**Figure 1**). The first of these mutants, hereafter termed NT, contains the N-terminus of ataxin-1 up to the start of the polyQ tract. Its behaviour was compared with that of a mutant (termed Atx1ΔNT) that excludes the region preceding the polyQ (30Qs) tract. The results from the whole analysis are summarized in **Table 1**.

As expected, wild-type ataxin-1 fused to YFP readily formed nuclear foci (**Figures 2A and B**). The YFP fusions of ataxin-1 constructs were similar in expression pattern to equivalent constructs that lacked YFP fusion and were stained with antibodies (data not shown), proving that the presence of YFP does not influence the data. The NT construct showed a diffused pattern of expression, demonstrating that this region is not involved in foci formation (**Figure 2C**). Addition of the polyQ tract to the N-terminal region (construct named NTQ) did not alter the behaviour of the cells (**Figure 2D**). We observed that constructs Atx1ΔNTQ and Atx1ΔNT were both able of forming foci (**Figures 2E and F**).

The observation that Atx1ΔNTQ, which lacks the polyQ tract, is able of foci formation demonstrates that polyQ region is not *per se* a foci forming factor. These results thus indicate that the C-terminus of ataxin-1 alone is involved in foci formation which does not involve the polyQ tract.

The AXH domain is insufficient to form foci but needs N-terminal extension

In order to further map the region required for nuclear foci formation, we expressed deletion mutants from the C-terminal region of ataxin-1 fused with YFP. We first expressed the region starting at the AXH domain and ending at the last residue of ataxin-1 (AXH2End, residues 562-816), which also contains the endogenous Nuclear Localisation Signal (NLS). As expected, this protein was mostly nuclear, but expressed itself in a diffused pattern (**Figures 3A and B**). A diffused pattern of nucleo-cytoplasmic expression was also observed for a construct with the AXH domain alone starting at amino acids ASPAA and comprising residues 562-689, termed AXH (**Figures 1, 3C and D**). Foci formation was observed instead when the AXH2End construct was N-terminally extended (residues 410-816, termed TLND2End (where TLND represents the N-terminal amino acid sequence of the construct) (**Figures 3E and F**).

These results thus suggest that the aggregation-prone AXH domain does not have a predominant role in foci formation by its own.

Evidence for the self-association prone CT2AXH motif

Since TLND2end formed foci while AXH2End did not, we next expressed the TLND2AXH region (residues 410-561) as YFP fusion to analyse if this is independently capable of foci formation. We observed that this construct formed foci that were, however, smaller in size as well as in number (**Figures 4A-C**). N-terminal extension of TLND2AXH (i.e. residues 221-561, construct CT2AXH) showed that the CT2AXH construct enhances foci formation ability (**Figures 4D and E**). The foci in both instances were mostly extra nuclear, which is not surprising as this region is not known to possess a functional NLS. C-terminal addition of SV40 NLS to CT2AXH resulted in exclusively nuclear foci formation (**Figures 4F and G**).

Lastly, deletion of the CT2AXH region from full-length YFP ataxin-1 (construct Atx1ΔCT2AXH) abolished foci formation (**Figures 4H and I**).

These results show that foci formation takes place independently from the AXH domain and that the nuclear localization signal has an influence on foci localisation.

Ataxin-1 contains dual dimerization motifs

The isolated AXH domain is known to dimerize in vitro (de Chiara et al., 2003; Chen et al., 2004; de Chiara et al., 2005; de Chiara et al., 2013a). Dimerization rather than other forms of self-association, could then be the seeding event for foci formation. Since nothing is known about the region N-terminally upstream to the AXH domain, we further characterized the TLND2AXH motif (residues 410-561) by analytical size exclusion chromatography (SEC) techniques to better understand the relationship between foci formation and the properties of the individual domains. Analytical gel-filtration chromatograms indicate that, in analogy with the AXH domain, the construct TLND2AXH is in equilibrium between two species which have an elution volume compatible with that of a monomer and a dimer. Higher retention volumes are observed for TLND2AXH as compared to AXH. This is justified by the elongated shape of the putatively unfolded TLND2AXH construct as compared to the compact fold of the AXH domain (Chen et al., 2004). The elution volume (12.7 ml) of the higher molecular weight species of TLND2AXH is anyway significantly smaller that expected for a trimer (48 kDa) or a tetramer (64 kDa).

These results provide solid evidence of the existence of a newly identified self-association region within ataxin-1 that is independent from the AXH domain.

The two distinct dimerization motifs are independently able of self-association in cells

To complement these *in vitro* studies of dimerization, we next tested the self-association regions identified in cultured cells and explored if they are capable of direct interaction leading to dimerization/self-association also in cell. To verify that the full-length ataxin-1 protein is indeed capable of self-association, we expressed full-length non-expanded ataxin-1 as CFP and YFP fusions and carried out FRET analysis. Self-association of ataxin-1 was evident from positive FRET signal (**Figures 6A-F**). We observed comparable FRET signals both when full-length ataxin-1 was expressed as C-terminal fusion to CFP (CFP-C-Atx1, **Figure 6A**) and YFP (YFP-C-Atx1**, Figure 6B**) and when ataxin-1 was C-terminal to CFP (CFP-C-Atx1, **Figure 6D**) and N-terminal to YFP (YFP-N-Atx1, **Figure 6E**). This suggests that the position of the fluorophore in ataxin-1 does not influence the FRET signal significantly.

We then expressed the newly identified dimerization motif TLND2AXH as CFP and YFP fusions. Self-association was evident in FRET experiments using the TLND2AXH construct (**Figures 6P-R**). As expected, the N-terminal extended form of TLND2AXH (CT2AXH) was also found to interact directly in cells (**Figures 6J-L**). Similarly, we carried out FRET analysis with CFP and YFP fusions of the AXH domain The results confirmed direct interaction between the YFP and CFP fusion proteins (**Figures 6M-O**).

Testing the effects of destabilization of AXH dimerization in cell

Finally, we used the FRET based approach to test the hypothesis that stabilization of the AXH domain into its monomeric form could result in reduction of protein aggregation. We used FRET analysis on co-expressed ataxin-1 YFP vs ataxin-1 CFP where ataxin-1 YFP plasmid also expressed a Capicua (CIC) peptide (residues 34-48 of the protein that we know to interact with the AXH domain with high affinity and to force it in a monomeric form (de Chiara et al., 2013b). Unfortunately, we were unable to verify the effect of the peptide since

the antibodies raised against it did not recognize the peptide (data not shown) preventing confirmation of peptide expression.

We resorted to a different strategy as a proof of principle. We have recently reported that mutation of a glycine at position 567 keeps the AXH domain in a predominantly monomeric form (de Chiara et al., 2013a). We thus tested if self-association in cells is affected by this mutation. We reasoned that a direct comparison is possible as this is only a point mutation which is unlikely to influence FRET data. We carried out a FRET analysis using the CFP ataxin-1 567 mutant and YFP-wild-type ataxin-1. Interestingly, we observed a significant reduction in the FRET signal (CFP 567 Atx1 versus YFP wt Atx1, **Figures 6G-I and 7**). This result suggests that identifying and manipulating vulnerable regions of ataxin-1 could be a tool to reduce self-association and possibly also have an effect on ataxin-1 aggregation. The corrected FRET efficiencies obtained with the different protein pairs and combined from different photo-bleaching experiments were calculated and are summarised in **Figure 7**.

We can thus conclude that both dimerization domains of ataxin-1 contribute to the self-interaction of the protein in cell.

Discussion

One aspect that distinguishes ataxin-1 from most other proteins is its ability to form small dense nuclear bodies (Skinner et al., 1997; Matilla et al., 1997). These bodies have been variously described as nuclear structures (Skinner et al., 1997), foci (Tsai et al., 2004), inclusions (Dovey et al., 2004), nuclear accumulations (Krol et al, 2008), or aggresomes (Latonen, 2011) with little consensus on the terminology used. Here, we preferred to name these structures foci as they are formed not just by the mutant expanded protein but also by the non-expanded protein or even by ataxin-1 without the incriminating polyQ tract (Tsai et al., 2004*)*. This is in agreement with the observations of nuclear structures both for expanded

and non-expanded ataxin-1 which only differed in size (Skinner et al, 1997). Regardless of the terminology, there is little doubt that these ataxin-1 structures are important in the normal as well as in pathological aspects of ataxin-1 function as various functional partners have been shown to associate with ataxin-1 within these bodies *(*Matilla et al., 1997; Chen et al., 2003; Mizutani et al., 2005; Menon et al., 2012*).* The small nuclear foci have been shown to further merge into larger bodies and this phenomenon is accelerated by polyQ expansion (Krol et al., 2008*).* Therefore the foci might also serve as seeding ground for aggregate formation. These observations suggest that new insights into foci formation events and identification of the regions responsible for this phenomenon could help not only the elucidation of the normal function of ataxin-1, but also the development of therapeutic strategies.

Our *in situ* investigations have now revealed that non-expanded ataxin-1 has two self-association motifs. Both AXH domain and the TLND2AXH motif are able to self-associate in transfected cells, as shown by FRET analysis. An earlier description of ataxin-1 self-association had identified this property almost exclusively with the AXH domain (Burright et al., 1997). This incorrect assumption has lead subsequent investigators to describe the self association region as partially overlapping the AXH domain (see for instance Krol et al., 2008). We now have clearly shown that this is not the case. FRET analysis, compared to co-localisation analysis, is capable of better demonstrating direct protein-protein interaction and is highly specific for self-association independently from the presence of other macromolecules. We have shown that both the non-overlapping TLND2AXH and AXH domains are *independently* capable of self-association while the former but not the latter is essential for foci formation. These observations are further supported by *in vitro* analysis of the dimerization properties of these motifs. Interestingly, gel filtration analysis demonstrates that the TLND2AXH motif is a dimer in equilibrium with the monomer, much like the AXH

domain itself (de Chiara et al., 2013a). Collectively, these results reiterate the importance of non-polyQ elements in the ataxin-1 functions and suggest that the dimerization observed for the AXH domain is an on-pathway event to aggregation.

In the attempt to define the relationship between dimerization and self-association, we also questioned if events that potentially reduce dimerization of individual motifs are able to influence the self-association tendency of ataxin-1 as measured by FRET analysis. In light of a recent report (Kim et al., 2013) and of our own findings (de Chiara et al., 2013b), we reasoned that a CIC peptide similar to the one used in our studies (de Chiara et al., 2013b) might reduce the self-association of ataxin-1. We therefore tried to do FRET analysis of CFP ataxin-1 in the presence of the CIC peptide (or a control scrambled peptide) expressed from a pIRES vector that also expressed YFP ataxin-1. However, we were unable to confirm the expression of the peptides as the antibodies raised against them were not effective. As an alternative to test our hypothesis, we carried out a FRET analysis using an ataxin-1 single mutant (A567G). A similar mutation in the AXH domain has been shown to keep the AXH domain in a predominantly monomeric form *in vitro* (de Chiara et al., 2013a). The FRET analysis between ataxin-1 567 mutant and ataxin-1 wild-type protein indicated a significantly lower FRET signal compared to wild-type/wild-type ataxin-1 FRET. Therefore, the AXH domain does not seem to contribute significantly in foci formation but has a role in self-association in agreement with previous data which showed that deletion in full-length ataxin-1 of the domain reduces intracellular aggregation (de Chiara et al., 2005). Our results provide a proof of principle of the potential effectiveness that can be achieved by disrupting ataxin-1 dimerization.

Conclusions

In conclusion, our study contributes to clarify the self-association properties of ataxin-1 and the relationship between these and the dimerization observed at the level of individual domains. This information may be used in further studies to probe the effect of the CIC interactions on aggregation and be helpful for designing new approaches to SCA1 therapy.

Acknowledgements

References

Arrasate M, Finkbeiner S. 2012. Protein aggregates in Huntington's disease. *Experimental Neurology* 238:1-11.

Blum ES, Schwendeman AR, Shaham S. 2013. PolyQ disease: misfiring of a developmental cell death program? *Trends in Cell Biology* 23:168-74.

Burright EN, Davidson JD, Duvick LA, Koshy B, Zoghbi HY, Orr HT. 1997. Identification of a self-association region within the SCA1 gene product, ataxin-1. *Human Molecular Genetics* 1997 6:513-8.

Cummings CJ, Mancini MA, Antalffy B, DeFranco DB, Orr HT, Zoghbi HY. 1998 Chaperone suppression of aggregation and altered subcellular proteasome localization imply protein misfolding in SCA1. *Nature Genetics* 19:148-154.

Cummings CJ, Orr HT, Zoghbi HY. 1999. Progress in pathogenesis studies of spinocerebellar ataxia type 1. P*hilosophical Transactions of the Royal Society of London B Biological Sciences*. 354:1079-1081.

Chen HK, Fernandez-Funez P, Acevedo SF, Lam YC, Kaytor MD, Fernandez MH, Aitken A, Skoulakis EM, Orr HT, Botas J, Zoghbi HY. 2003. Interaction of Akt-phosphorylated ataxin-1 with 14-3-3 mediates neurodegeneration in spinocerebellar ataxia type 1. *Cell* 113:457-68.

Chen YW, Allen MD, Veprintsev DB, Löwe J, Bycroft M. 2004. The structure of the AXH domain of spinocerebellar ataxin-1. *Journal of Biological Chemistry* 279:3758-3765.

de Chiara C, Giannini C, Adinolfi S, de Boer J, Guida S, Ramos A, Jodice C, Kioussis D, Pastore A. 2003. The AXH module: an independently folded domain common to ataxin-1 and HBP1. *FEBS Letters* 551:107-12.

de Chiara C, Menon RP, Dal Piaz F, Calder L, Pastore A. 2005. Polyglutamine is not all: the functional role of the AXH domain in the ataxin-1 protein. *Journal of Molecular Biology* 354:883-893.

de Chiara C, Rees M, Menon RP, Pauwels K, Lawrence C, Konarev PV, Svergun DI, Martin SR, Chen YW, Pastore A. 2013a. Self-assembly and conformational heterogeneity of the AXH domain of ataxin-1: an unusual example of a chameleon fold. *Biophysical Journal* 104:1304-13.

de Chiara C, Menon RP, Kelly G, Pastore A. 2013b. Protein-protein interactions as a strategy towards protein-specific drug design: the example of ataxin-1. *PLoS One* 8:e76456.

de Chiara C, Pastore, A. 2014. Kaleidoscopic protein-protein interactions in the life and death of ataxin-1: New strategies against protein aggregation. *Trends in Neurology* (in press)

Dovey CL, Varadaraj A, Wyllie AH, Rich T. 2004. Stress responses of PML nuclear domains are ablated by ataxin-1 and other nucleoprotein inclusions. *Journal of Pathology* 203:877-883.

Ellisdon AM, Thomas B, Bottomley SP. 2006. The 2-stage pathway of ataxin-3 fibrillogenesis involves a polyglutamine-independent step. *J. Biol. Chem.* 281:16888-16896.

Gales, L., L. Cortes, C. Almeida, C. V. Melo, M. do Carmo Costa, P. Maciel, D. T. Clarke, A. M. Damas, and S. Macedo-Ribeiro. 2005. Towards a Structural Understanding of the Fibrillization Pathway in Machado-Joseph's Disease: Trapping Early Oligomers of Non-expanded Ataxin-3. *J Mol Biol* 353:642-654.

Goold R, Hubank M, Hunt A, Holton J, Menon RP, Revesz T, Pandolfo M, Matilla-Dueñas A. 2007. Down-regulation of the dopamine receptor D2 in mice lacking ataxin 1. *Human Molecular Genetics* 1617:2122-2134.

Hlavackova V, Zabel U, Frankova D, Bätz J, Hoffmann C, Prezeau L, Pin JP, Blahos J, Lohse MJ. 2012. Sequential inter- and intrasubunit rearrangements during activation of dimeric metabotropic glutamate receptor 1. *Science Signaling* 5:ra59.

Itoh Y, Palmisano R, Anilkumar N, Nagase H, Miyawaki A, Seiki M. 2011. Dimerization of MT1-MMP during cellular invasion detected by fluorescence resonance energy transfer. *Biochemical Journal* 440:319-26.

Kim E, Lu HC, Zoghbi HY, Song JJ. 2013. Structural basis of protein complex formation and reconfiguration by polyglutamine disease protein Ataxin-1 and Capicua. *Genes &Development* 27:590-595.

Klement IA., Skinner PJ, Kaytor MD, Yi H, Hersch SM, Clark, HB, Zoghbi HY, Orr HT. 1998. Ataxin-1 nuclear localization and aggregation: role in polyglutamine-induced disease in SCA1 transgenic mice. *Cell* 95:41-53.

Krol HA, Krawczyk PM, Bosch KS, Aten JA, Hol EM, Reits EA. 2008. Polyglutamine expansion accelerates the dynamics of ataxin-1 and does not result in aggregate formation. *PLoS One* 3:e1503.

Lam YC, Bowman AB, Jafar-Nejad P, Lim J, Richman R, Fryer JD, Hyun ED, Duvick LA, Orr HT, Botas J, Zoghbi HY. 2006. ATAXIN-1 interacts with the repressor Capicua in its native complex to cause SCA1 neuropathology. *Cell* 127: 1335-1347.

Latonen L. 2011. Nucleolar aggresomes as counterparts of cytoplasmic aggresomes in proteotoxic stress. Proteasome inhibitors induce nuclear ribonucleoprotein inclusions that accumulate several key factors of neurodegenerative diseases and cancer. *Bioessays* 33:386-395.

Lee S, Hong S, Kim S, Kang S. 2011. Ataxin-1 occupies the promoter region of E-cadherin in vivo and activates CtBP2-repressed promoter. *Biochimica et Biophysica Acta* 1813:713–722.

Masino, L., Nicastro, G., Menon, R. P., Dal Piaz, F., Calder, L. & Pastore, A. (2004). *Journal of molecular biology* 344:1021-1035.

Matilla A, Koshy BT, Cummings CJ, Isobe T, Orr HT, Zoghbi HY. 1997. The cerebellar leucine-rich acidic nuclear protein interacts with ataxin-1. *Nature* 389:974-978.

Matilla-Dueñas A, Goold R, Giunti P. 2008. Clinical, genetic, molecular, and pathophysiological insights into spinocerebellar ataxia type 1. *Cerebellum* 7:106-114.

Matthews HK, Marchant L, Carmona-Fontaine C, Kuriyama S, Larraín J, Holt MR, Parsons M, Mayor R. 2008. Directional migration of neural crest cells in vivo is regulated by Syndecan-4/Rac1 and non-canonical Wnt signaling/RhoA. *Development* 135:1771-1780.

Menon RP, Soong D, de Chiara C, Holt MR, Anilkumar N, Pastore A. 2012. The importance of serine 776 in Ataxin-1 partner selection: a FRET analysis. *Scientific Reports* 2:919.

Menon RP, Nethisinghe S, Faggiano S, Vannocci T, Rezaei H, Pemble S, Sweeney MG, Wood NW, Davis MB, Pastore A, Giunti P. 2013. The role of interruptions in polyQ in the pathology of SCA1. *PLoS Genetics* 9:e1003648.

Mizutani A, Wang L, Rajan H, Vig PJ., Alaynick WA., Thaler JP, Tsai CC. 2005. Boat, an AXH domain protein, suppresses the cytotoxicity of mutant ataxin-1. *EMBO Journal* 24: 3339-3351.

Okazawa H, Rich, T, Chang A, Lin X, Waragai M, Kajikawa M, Enokido Y, Komuro A, Kato S, Shibata M, Hatanaka H, Mouradian MM, Sudol M, Kanazawa I. 2002. Interaction between mutant ataxin-1 and PQBP-1 affects transcription and cell death. *Neuron* 34:701–713.

Osmand AP, Berthelier V, Wetzel R. 2006. Imaging Polyglutamine Deposits in Brain Tissue. Methods in Enzymology 412:106-122.

Orr HT, Chung MY, Banfi S, Kwiatkowski TJ Jr, Servadio A, Beaudet AL, McCall AE, Duvick LA, Ranum LP, Zoghbi HY. 1993. Expansion of an unstable trinucleotide CAG repeat in spinocerebellar ataxia type 1. *Nature Genetics* 4:221–226.

Placone J, Hristova K. 2012. Direct assessment of the effect of the Gly380Arg achondroplasia mutation on FGFR3 dimerization using quantitative imaging FRET. PLoS One. 7:e46678.

Robertson AL, Bottomley SP. 2012. Molecular pathways to polyglutamine aggregation. *Advances in Experimental Medicine and Biology* 769:115-24.

Serra HG, Duvick L., Zu T, Carlson K, Stevens S, Jorgensen N, Lysholm A, Burright E, Zoghbi HY, Clark HB, Andresen JM Orr HT. 2006. RORalpha-mediated Purkinje cell development determines disease severity in adult SCA1 mice. *Cell* 127:697–708.

Skinner PJ, Koshy BT, Cummings CJ, Klement IA, Helin K, Servadio A, Zoghbi HY, Orr HT. 1997. Ataxin-1 with an expanded glutamine tract alters nuclear matrix-associated structures. *Nature* 389:971-984.

Tsai CC, Kao HY, Mitzutani A, Banayo E, Rajan H, McKeown M, Evans RM. 2004. Ataxin-1, a SCA1 neurodegenerative disorder protein, is functionally linked to the silencing mediator of retinoid and thyroid hormone receptors. *Proceedings of the National Academy of Sciences USA* 101:4047-4052.

Tsuda H, Jafar-Nejad H, Patel AJ, Sun Y, Chen HK, Rose MF, Venken KJ, Botas J, Orr HT, Bellen HJ, Zoghbi HY. 2005. The AXH domain of Ataxin-1 mediates neurodegeneration through its interaction with Gfi-1/Senseless proteins. *Cell* 122:633-644.

Verbeek DS, van de Warrenburg BP. 2011. Genetics of the dominant ataxias. *Seminars in Neurology* 31:461-9.

Zoghbi HY, Orr HT. 1995. Spinocerebellar ataxia type 1. *Seminars in Cell Biology* 6:29-33.

Legends to Figures:

Figure 1: Summary of the ataxin-1 constructs used in the present study.

Full-length ataxin-1 protein is represented by a black line. The positions of the polyQ tract, the AXH domain and NLS are explicitly indicated.

Figure 2: Identifying the region responsible for foci formation in ataxin-1.

Various deletion constructs of ataxin-1 were expressed as YFP fusion proteins in COS cells. A) Full-length ataxin-1 30Q-YFP. Overlay with Dapi is shown in B. Expression analysis shows a diffused expression pattern in cells expressing ataxin-1 N terminal regions without (C) or with the polyQ tract (D). In contrast, cells expressing the C-terminal regions either without (E) or with (F) the polyQ tract readily formed foci.

Figure 3: AXH domain is not involved in foci formation.

A YFP construct starting at the ataxin-1 AXH domain and ending at the last ataxin-1 amino acid (AXH2END) was expressed as a YFP fusion in COS cells (A and B). These cells showed a diffused YFP fluorescence which was nuclear, as evidenced by DAPI overlay (B). YFP tagged AXH domain also failed to form foci (C and D). Upon N-terminal extension of the AXH2END construct to include further residues starting from amino acids TLND, nuclear foci formation was observed (**Figure 4E and F**). YFP fluorescence in left panels is overlaid with DAPI in right panels.

Figure 4: Foci forming analysis of the CT2AXH region.

Residues TLND to AXH from ataxin-1 in fusion with YFP forms small foci that are extra nuclear (**panels A and B**). One cell from the image is enlarged in C for clarity. N terminal extension of this region where the construct started after the polyQ tract (CT2AXH) formed

larger foci which also were extra nuclear (**panels C, D and E**). Addition of an NLS to this construct resulted in nuclear foci formation (**panels F and G**). Deletion of CT2AXH from ataxin-1 resulted in diffused expression of the protein (**panels H and I**). A,D F and H show YFP fluorescence. YFP fluorescence is overlaid with DAPI in B, C, E, G and I.

Figure 5: Analytical size exclusion chromatography.

Analytical gel-filtration chromatograms of AXH (continuous line) and TLND2AXH (dotted line) constructs. The position of molecular weight markers is indicated for comparison. Calculated molecular weights are 13.9 kDa for AXH and 16 kDa for TLND2AXH.

Figure 6: 'Rainbow' pseudocolour look-up table (LUT)-encoded pre- and post-bleach images of CFPand YFP fusion proteins.

Magnified crops of both CFP and YFP signals in the bleach region (black circles) are depicted for pre- and post-bleach for each FRET pair (C,F,I,L,O and R). All scale bars are 5 μm. The FRET pairs are,
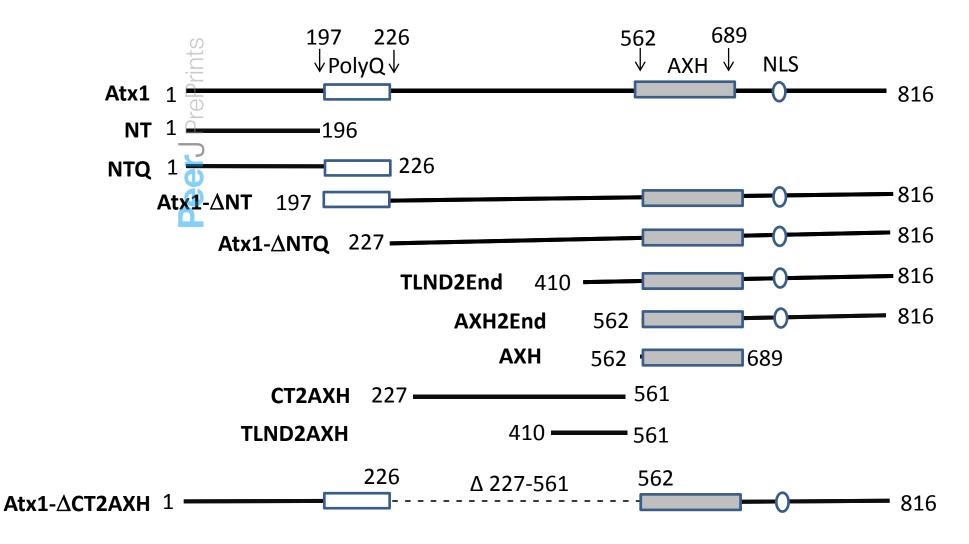
A-C) CFP-C--Atx1 vs YFP-C-Atx1; A) CFP fluorescence, B) YFP fluorescence

D-F) CFP-C-Atx1 vs YFP-N-Atx1; D) CFP fluorescence, E) YFP fluorescence

G-I) CFP-567-Atx1 vs YFP-wt-Atx1; G) CFP fluorescence, H) YFP fluorescence

J-L) CFP-CT2AXH vs YFP-CT2AXH; J) CFP fluorescence , K) YFP fluorescence

M-O) CFP-AXH vs YFP-AXH; M) CFP fluorescence, N) YFP fluorescence

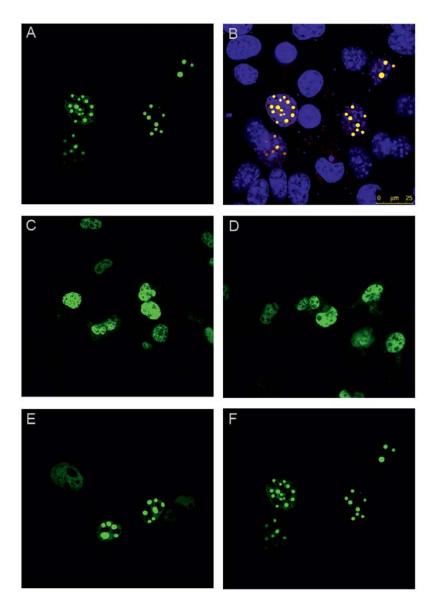P-R) CFP-TLND2AXH vs YFP-TLND2AXH P) CFP fluorescence, Q) YFP fluorescence

Figure 7: Box and whisker plots depicting population distribution of percentage corrected FRET and showing maximum, minimum, upper & lower quartiles, and sample median.
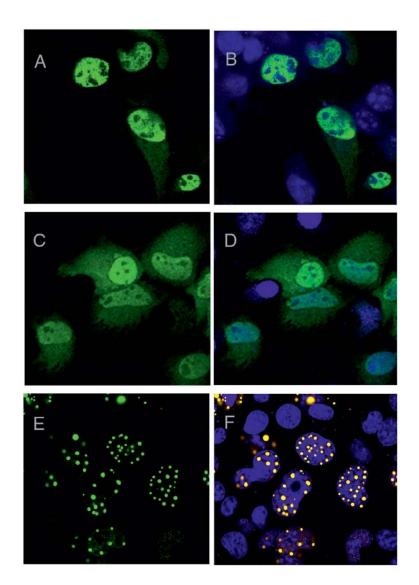
The individual FRET pairs are shown in the X axis. These are: 1) CFP-C--Atx1 vs CFP-C-Atx1; 2) CFP-C-Atx1 vs YFP-N-Atx1; 3) CFP-567-Atx1 vs YFP-wt-Atx1 4) CFP-CT2AXH vs YFP-CT2AXH; 5) CFP-AXH vs YFP-AXH; 6) CFP-TLND2AXH vs YFP-TLND2AXH Means +/- standard errors, rounded to one decimal place, are shown above each boxplot. Statistical significance bars are shown and represent results of unpaired t-tests of mean difference = 0 and represent number of individual bleach events pooled from at least 4 individual cells.
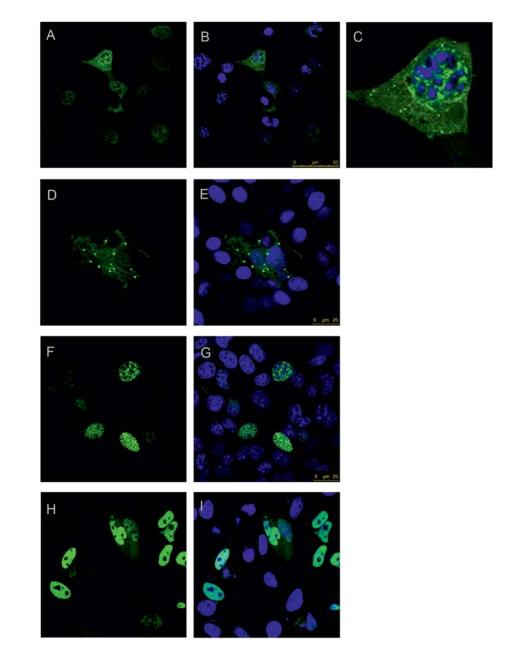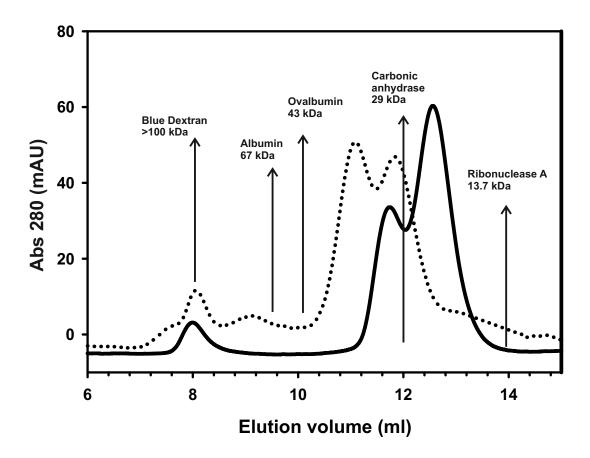
Table 1: Ataxin-1 constructs and their foci forming abilities.

Construct	Amino acids involved	Foci formation	Foci Localization
Ataxin-1 wild-type	1-816	Yes	Nucleus
NT	1-196	No	N/A
NTQ	1-226	No	N/A
Atx1ΔNT	197-816	Yes	Nucleus
Atx1ΔNTQ	227-816	Yes	Nucleus
TLND2END	410-816	Yes	Nucleus
AXH2END	562-816	No	N/A
AXH	562-689	No	N/A
CT2AXH	227-561	Yes	Cytoplasm
TLND2AXH	410-561	Yes	Cytoplasm
Atx1ΔCT2AXH	Deletion of 227-561	No	N/A

Figure 1

Figure 2

Figure 3

Figure 4

Figure 6

Figure 7